

Magneto-optical effects and rf magnetic field detection in cold rubidium atoms

Krystian Sycz, Adam M. Wojciechowski, and Wojciech Gawlik

Jagiellonian University, Reymonta 4, 30-059 Kraków, Poland

E-mail: a.wojciechowski@uj.edu.pl

Abstract. We present the results of our latest experiments on atomic coherences in cold atoms. Interaction of atoms with a near-resonant, linearly polarized light leads to an effective creation of long-lived ground-state Zeeman coherences which is observed through the nonlinear Faraday effect or free induction decay signals of the Larmor precession. Both optically and radio-frequency induced Zeeman coherences are observed, with relaxation rates around a 100 Hz.

1. Introduction

Ever since the first experiments with laser cooling of neutral atoms, there is a growing interest in the field of cold and ultra-cold diluted gases, see, e.g., references [1, 2, 3]. Due to the slowed down motion and confinement, atom observation time can be as long as minutes, which results in the extraordinary stability of atomic clocks [4, 5], as well as the great sensitivity of atomic interferometers [6]. Moreover, cold atomic samples have been widely used for detection of electric and magnetic fields [7, 8, 9, 10, 11, 12, 13]. State-of-the-art experiments exhibit now quantum limited sensitivities, see, e.g., reference [14].

In this work we report on our latest experiments on nonlinear magneto-optical effects in laser-cooled rubidium samples released from a magneto-optical trap (MOT) [15]. Such experiments in a MOT present both unique opportunities and challenges compared to those performed in vapor cells at room temperatures. The most obvious difference is the greatly reduced velocity of atoms that brings the Doppler broadening below the homogeneous width of the hyperfine transitions. On the other hand, however, the trapping and cooling electromagnetic fields need to be turned off during the measurements because they significantly disturb atoms. Once released from the trap atom cloud spreads out and undergoes a freefall which limit the available observation time to about 20 milliseconds. The duty-cycle (measurement bandwidth) is also limited because the atoms need to be recaptured before the next measurement can be performed.

Interaction of atoms with a near-resonant, linearly polarized light leads to an effective creation of long-lived ground-state Zeeman coherences [16] which can be observed through the nonlinear, or paramagnetic Faraday effect [17]. Optical nonlinearity that results from existence of ground-state coherences allows for precision magnetometry of near-zero magnetic fields [18]. Additionally, by employing the amplitude-modulated optical rotation [19] it is possible to measure also higher magnetic fields up to the geophysical range [15]. Moreover, Zeeman coherences form a versatile tool for studying superposition states [20] which are vital to fundamental atomic physics and quantum information. In this work, we demonstrate the dynamics of coherent superposition states under the influence of laser and magnetic fields. Our



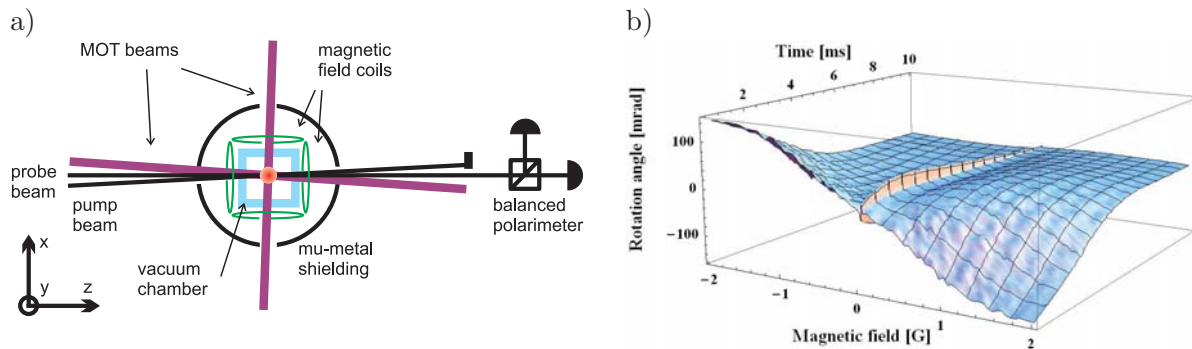


Figure 1. a) Schematic plot of the experimental setup. b) Faraday rotation in the atomic sample released from the MOT as a function of time and magnetic field B . Wide resonance is the linear, whereas the central, narrow structure around $B = 0$ is the nonlinear effect. Decay of the total signal corresponds to the loss of atoms due to the combined effect of their freefall, cloud expansion, optical pumping and magnetic field inhomogeneities.

experiments show that high rotation angles of above ten degrees and coherence lifetimes of a few milliseconds can be achieved with cold atoms released from the MOT in a simple magnetically shielded setup.

2. The experiment

In our experiments we prepare cold atomic samples of about 10^8 ^{85}Rb atoms at the temperature of the order of 50-100 μK in a standard vapor-pressure-loaded MOT. Atoms are then released from the trap by switching off the trapping laser beams and the quadrupole magnetic field. During the freefall of the cloud, a uniform magnetic field and a weak probing beam are applied along the z axis [15]. Additionally, a resonant pumping beam along the z direction is used for preparation of the atomic state by optical pumping means. Polarization of the pumping beam is set either to the linear or the circular one, depending on the experiment. The probe beam is linearly polarized along y direction and the rotation of its polarization plane is recorded in time using a balanced polarimeter. Subsequently the trap is reloaded and the next measurement is performed for a different value of the Faraday magnetic field. In this way the magneto-optical rotation signals are recorded versus time and magnetic-field (Fig. 1).

To alleviate the effect of stray magnetic fields we shield the experimental vacuum chamber with a simple, single-layer μ -metal shielding. The magnetic shield consists of a cylinder with two end caps and a set of holes in three orthogonal directions x, y, z for the MOT, pumping and probing beams. Inside the shield the MOT-quadrupole field coils are mounted, as well as the set of coils that allows for application of the extra magnetic fields and their gradients in the three directions. The shield, despite its simplicity, provides a shielding factor of the order of 20 and, more importantly, reduces the time by which the quadrupole field can be switched off. This effect is attributed to the fact, that massive optical mounts in the vicinity of the MOT trap are shielded and the contribution of the generated eddy currents is diminished.

3. Experimental results

3.1. Nonlinear Faraday effect

When a linearly polarized, resonant laser beam is directed at the atomic cloud in a longitudinal magnetic field, its polarization plane undergoes rotation due to the para- and diamagnetic Faraday effects. After switching off the MOT, initial atomic population distribution in our experiments can be regarded as uniform over Zeeman substates with no Zeeman coherences in

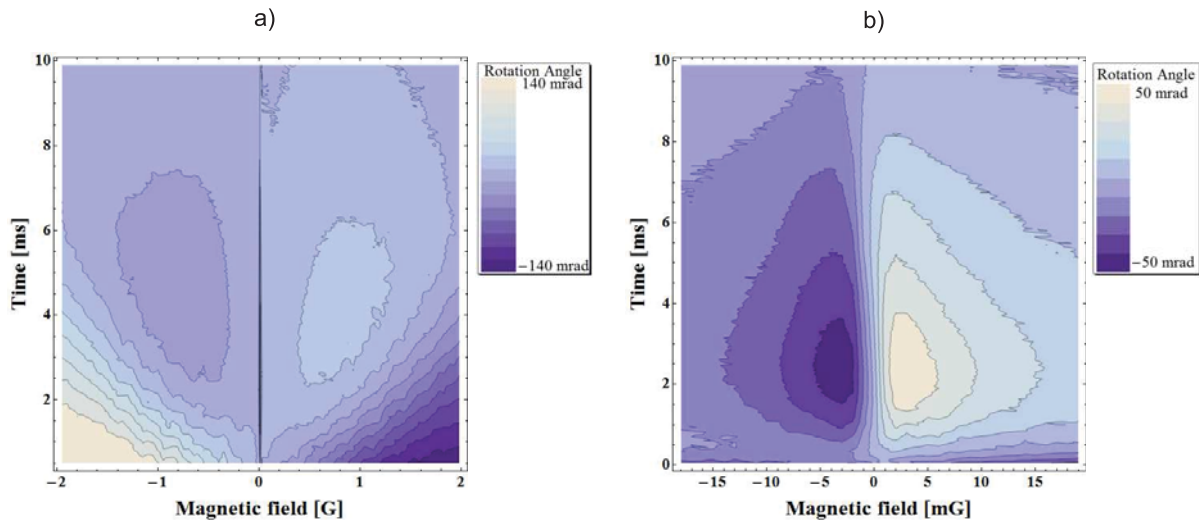


Figure 2. Contour plots of the nonlinear Faraday rotation signal with a single, probe beam of $2 \mu\text{W}/\text{mm}^2$ intensity in a wide (a) and narrow (b) magnetic field range. The width of the NFE resonance is 6.5 mG

the $F = 3$ manifold of the $5^2S_{1/2}$ ground state. However, application of the resonant laser beam may drastically change this distribution. The linearly polarized light creates an alignment in the ground state with no net magnetization, yet with Zeeman coherences evolving in the magnetic field. For a CW laser light, this results in a quasi-stationary (compared to the Larmor precession) rotation of the polarization angle, the nonlinear Faraday effect (NFE).

Typical magneto-optical rotation signal $\phi(B)$ obtained with a relatively weak probing beam ($\sim 2 \mu\text{W}/\text{mm}^2$), nearly resonant with the $F = 3 \rightarrow F' = 4$ transition of the ^{85}Rb D2 line is shown in Fig. 1. Signal decay with time is easily seen, and can be attributed to the combined effect of atom loss due to the freefall, cloud expansion (dilution) optical pumping, and inhomogeneous magnetic field. The wide dispersive structure around $B = 0$ is the linear Faraday effect (LFE) and has a width of ~ 20 G. Additionally, the signal exhibits a much narrower resonance, also centered around $B = 0$, which corresponds to the NFE. This effect can be understood in terms of optical pumping, and thus requires time to build-up, which is easily seen in Fig. 2. The width of the NFE resonance, typically ~ 1 mG, is much narrower than that of the LFE and corresponds to the lifetime of the $\Delta m = 2$ Zeeman coherences in the $F = 3$ ground state [17] (m being the magnetic quantum number).

The large amplitude of a few degrees and narrow width of the NFE resonance allows for precision magnetic field measurements. The magnetometric sensitivity improves when the NFE resonance width is reduced [18]. It is thus advantageous to keep the resonance width as narrow as possible, i.e., prolong the coherence lifetime. Special care has to be taken to achieve long coherence life-times, since any stray magnetic fields can shorten it. In the following subsection we discuss the pump-probe method we used for assessment of magnetic-fields compensation.

3.2. Pulsed pump experiments

The nonlinear Faraday Effect allows one to measure an averaged response of an ensemble of a cold atom ensemble to the applied magnetic fields. It is, however, possible to observe the dynamics of the system by using a relatively short ($\tau \ll 1/\omega_L$, where ω_L is the Larmor precession frequency) strong light pulse for creation of the desired atomic population distribution. After such a pulse, the evolution of the system is interrogated by measuring the polarization rotation of a weak

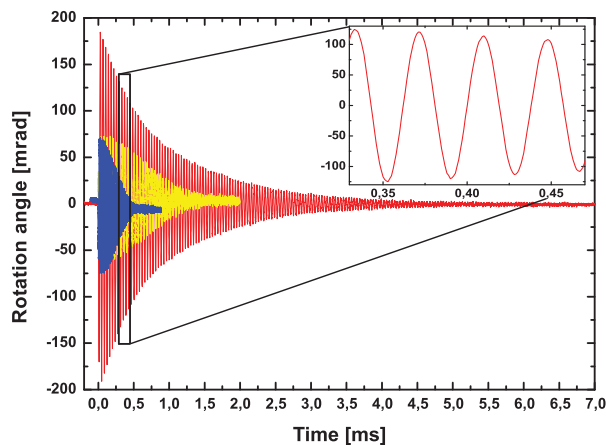


Figure 3. Comparison of the FID signals with and without magnetic shielding. The blue (shortest) and yellow (middle long) curves show data obtained in an unshielded chamber, with passive compensation of the ambient magnetic fields and additional compensation of the field gradients, respectively. The red (longest) curve was recorded in a shielded environment, where the measured decay time equals $\tau = 980 \mu\text{s}$. Notice the change of the FID signal envelope shapes.

probing beam.

By means of a σ^+ -polarized pump pulse propagating along the z direction we pump the atoms into the stretched state, $F = 3$, $m_F = 3$, assuming the quantization axis along the z -direction. We then apply a dc magnetic field B_x along the x axis which causes the atomic polarization to rotate around that field at a frequency proportional to its magnitude, i.e., Larmor frequency ω_L . The created distribution of atomic populations among the ground state Zeeman sublevels causes the polarization of a weak probe light to oscillate due to the paramagnetic Faraday effect, and this oscillation is recorded in the form of a free induction decay (FID) signal [7, 21, 22]. Such oscillations decay with a relaxation rate of Zeeman coherences, which is governed by several factors, including transverse magnetic fields, magnetic field instability and interaction with the probing light via absorption and AC Stark shifts.

The effect of stray magnetic field is shown in Fig. 3 where signals recorded with and without magnetic shielding are compared. Not only the coherence lifetime is prolonged in the shielded case, but also the envelope of the FID signal shows the exponential decay - a proof for the right magnetic field control. We were able to determine that after minimizing all other sources of decoherence we are left with the dephasing due to the spatial inhomogeneity of the applied magnetic field. Slight differences in the values of the B_x field across the atomic cloud are attributed to atoms from different parts of the sample experiencing precession at slightly deviated frequencies. The rate of such dephasing was measured to be $\gamma_x = 2\pi \cdot 160 \text{ Hz}$.

3.3. FID signals of Zeeman coherences

In a standard observation of FID signals, the sample is magnetized along one direction and then subjected to the precession around a perpendicularly oriented magnetic field, which provides the highest amplitude of the rotation signal. It is, however, possible to observe the FID spin polarization dynamics in an arrangement where the pump beam is propagating along the B-field direction, i.e., the natural geometry for the Faraday rotation experiments. Since Zeeman substates are the eigenstates of the magnetic field, it is only Zeeman coherences which evolve in time in such a realization.

To record FID signals associated with Zeeman coherences, we use a short pump pulse of the linearly polarized beam, which prepares the $F = 3$ ground-state $\Delta m = 2$ Zeeman coherences, and monitor time dependence of the rotation angle of the probe beam polarization. Examples of such dependence of FID signals on the magnetic field are shown in Fig. 4. Clearly visible are the hyperbolas of the constant phase of Larmor precession. Frequency of the Larmor precession tends to zero around the zero field (long oscillation period) and increases with the magnetic field

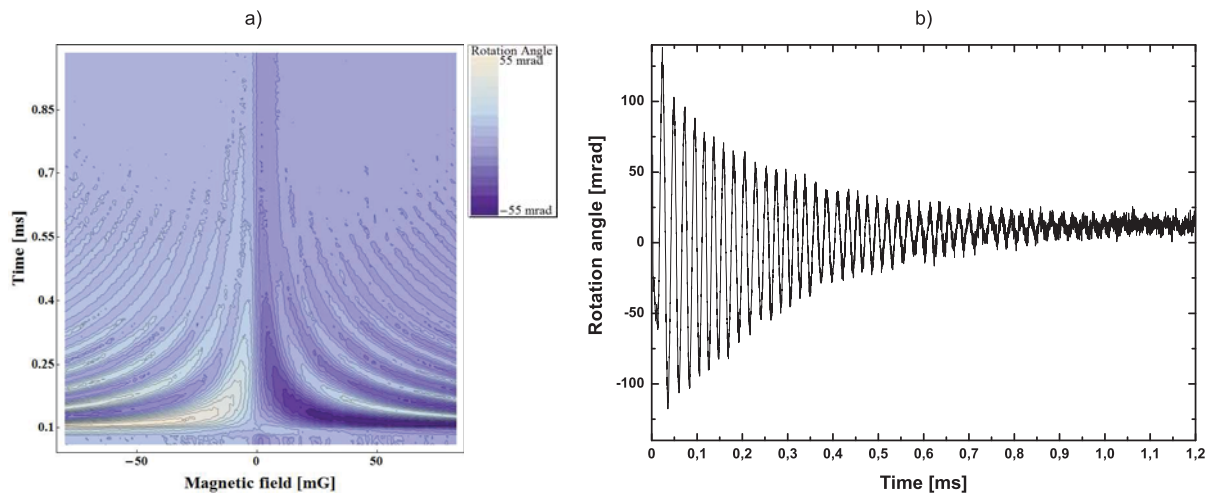


Figure 4. FID signals of the $\Delta m = 2$ atomic coherences prepared by a short pumping light pulse at $t = 0$. a) Contour plot of the rotation dependence on time and the magnetic field, b) coherences FID signal recorded for $B_z = 95$ mG.

magnitude.

3.4. Detection and measurements of the radio-frequency magnetic fields

By tuning the Zeeman splitting to resonance with an external radio-frequency field B_{rf} oscillating at the frequency ω_{rf} in the x direction we are able to observe resonant changes of the rotation angle. This happens provided that there is some initial inequality in atomic populations of given sublevels is established by optical pumping. These resonances can be applied for magnetometry in two ways: (i) the rf resonance frequency is taken as the measure of the dc magnetic field intensity B , (ii) the amplitude of resonance in the rotation amplitude can be used for measurement of the intensity of the rf field B_{rf} [23, 24].

For sufficiently strong amplitude B_{rf} , Rabi oscillations between neighboring Zeeman sublevels of the ground state manifold can be observed due to the paramagnetic Faraday rotation. By initially preparing atoms in the stretched state with a short σ^+ light pulse as described earlier, we are able to maximize the observed rotation angles.

Our present experimental setup is severely limited by a short lifetime of the MOT and cannot compete with other optical magnetometers in terms of sensitivity. Instead, we can use it for studies of a coherent interaction between cold atoms and various fields, like coherent evolution of atomic observables in the rf field. Figure 5 (a) depicts an example of Rabi oscillations recorded with rf field of 11 kHz frequency and 5.5 mG amplitude. The width of the rf rotation resonances is strongly power broadened. This allows observation of the dependence of the generalized Rabi frequency on the detuning of ω_{rf} from the exact Larmor frequency in the form of characteristic bending of the resonance features on a contour map [Fig. 5 (a)]. Rabi oscillations for lower rf field amplitude and with relaxation rate $\gamma_{\text{rf}}/2\pi \sim 50$ Hz are shown in Fig. 5 (b). It is worth noting that polarization rotation angle can easily reach hundreds of milliradians in an atomic cloud from a standard MOT.

4. Conclusions

We have demonstrated an ability to observe a coherent evolution of polarized atoms prepared in a magneto optical trap for times of the order of milliseconds and detection of dc and rf magnetic fields with high sensitivity. The present experimental setup is limited by a short

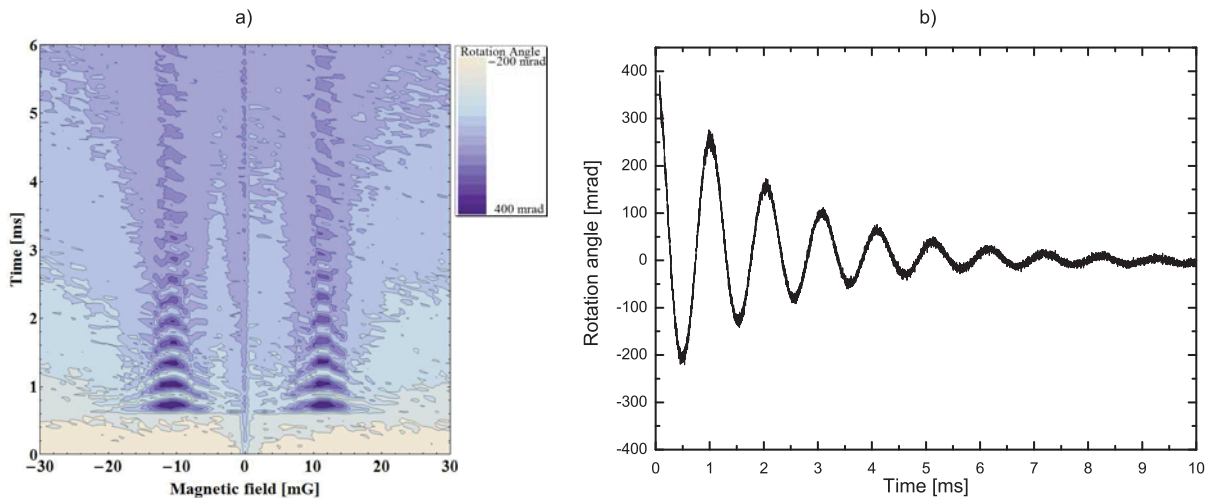


Figure 5. a) Contour plot of the polarization rotation dependence on time and a dc magnetic field showing Rabi oscillations induced by the rf magnetic field of frequency $\omega_{\text{rf}} = 2\pi \cdot 11$ kHz and amplitude $B_{\text{rf}} = 5.5$ mG switched on at $t \approx 0.6$ ms. b) Rotation signal for the resonance condition $\omega_L = \omega_{\text{rf}} = 2\pi \cdot 8.2$ kHz, $B_{\text{rf}} \approx 1.7$ mG.

lifetime of the MOT. The reported observations indicate, nevertheless, that the upgrade to a far-detuned optical dipole trap would significantly improve the lifetimes of the trapped atoms. Consequently, this would allow applications in sensitive magnetometry and studies of long-lived atomic superpositions states, including quantum degenerated samples.

Acknowledgments

Authors acknowledge financial support by the Foundation for Polish Science (Team Programme) and the National Science Centre (grant no. 2012/07/B/ST2/00251). AW acknowledges support by the Jagiellonian University within the SET project co-financed by the European Union.

References

- [1] Ketterle W, Durfee D and Stamper-Kurn D 1999 *Bose-Einstein condensation in atomic gases* Proceedings of the International School of Physics Enrico Fermi. Course CXL ed Inguscio M, Stringari S and Wieman C (IOS Press, Amsterdam) (*Preprint arXiv:cond-mat/9904034*)
- [2] Lewenstein M, Sanpera A, Ahufinger V, Damski B, Sen(De) A and Sen U 2007 *Advances in Physics* **56** 243
- [3] Ketterle W and Zwierlein M W 2008 *Ultracold Fermi Gases* Proceedings of the International School of Physics Enrico Fermi. Course CLXIV ed Inguscio M, Ketterle W and Salomon C (IOS Press, Amsterdam) (*Preprint 0801.2500*)
- [4] Katori H 2011 *Nature Photonics* **5** 203–210
- [5] Le Targat R et al 2013 *Nature Communications* **4** 2109
- [6] Dickerson S M, Hogan J M, Sugarbaker A, Johnson D M S and Kasevich M A 2013 *Phys. Rev. Lett.* **111**(8) 083001
- [7] Isayama T, Takahashi Y, Tanaka N, Toyoda K, Ishikawa K and Yabuzaki T 1999 *Phys. Rev. A* **59** 4836–4839
- [8] Franke-Arnold S, Arndt M and Zeilinger A 2001 *J. Phys. B* **34** 2527–2536
- [9] Labeyrie G, Miniatura C and Kaiser R 2001 *Phys. Rev. A* **64** 033402
- [10] Nash J and Narducci F A 2003 *Journ. Mod. Optics* **50** 2667
- [11] Wildermuth S, Hofferberth S, Lesanovsky I, Groth S, Krüger P, Schmiedmayer J and Bar-Joseph I 2006 *Appl. Phys. Lett.* **88** 264103
- [12] Vengalattore M, Higbie J M, Leslie S R, Guzman J, Sadler L E and Stamper-Kurn D M 2007 *Physical Review Letters* **98** 200801
- [13] Terraciano M L, Bashkansky M and Fatemi F K 2008 *Opt. Express* **16** 13062–13069

- [14] Sewell R J, Koschorreck M, Napolitano M, Dubost B, Behbood N and Mitchell M W 2012 *Phys. Rev. Lett.* **109**(25) 253605
- [15] Wojciechowski A, Corsini E, Zachorowski J and Gawlik W 2010 *Physical Review A* **81** 053420–0533424
- [16] Cohen-Tannoudji C 1999 *Frontiers in Laser Spectroscopy, Les Houches Summer School 1975* ed RBalian, Haroche S and Liberman S (North Holland) (*Preprint arXiv:cond-mat/9904034*)
- [17] Budker D, Gawlik W, Kimball D F, Rochester S M, Yashchuk V V and Weis A 2002 *Reviews of Modern Physics* **74** 1153–11201
- [18] Budker D, Kimball D F, Rochester S M, Yashchuk V V and Zolotarev M 2000 *Phys. Rev. A* **62**(4) 043403
- [19] Gawlik W, Krzemień L, Pustelny S, Sangla D, Zachorowski J, Graf M, Sushkov A O and Budker D 2006 *Applied Physics Letters* **88** 131108–131110
- [20] Gawlik W and Wojciechowski A 2011 *Optics and Spectroscopy* **111** 626–632
- [21] Takahashi Y, Shimizu T, Tanaka N, Honda K, Toyoda K and Yabuzaki T 1999 *Phys. Rev. A* **59**(5) 3761–3765
- [22] Behbood N, Martin Ciurana F, Colangelo G, Napolitano M, Mitchell M W and Sewell R J 2013 *Applied Physics Letters* **102**
- [23] Savukov I M, Seltzer S J, Romalis M V and Sauer K L 2005 *Phys. Rev. Lett.* **95**(6) 063004
- [24] Ledbetter M P, Acosta V M, Rochester S M, Budker D, Pustelny S and Yashchuk V V 2007 *Phys. Rev. A* **75**(2) 023405